Free energy of formation of zircon based on solubility measurements at high temperature and pressure

ROBERT C. NEWTON,[1] CRAIG E. MANNING,[1,*] JOHN M. HANCHAR,[2] AND CLINTON V. COLASANTI[1]

[1]Department of Earth and Space Sciences, University of California at Los Angeles, Los Angeles, California 90095, U.S.A.
[2]Department of Earth Sciences, Memorial University, St. Johns, Newfoundland A1B 3X5, Canada

ABSTRACT

The standard Gibbs energy of formation of zircon was constrained by measuring the solubility of silica in H_2O in equilibrium with zircon and baddeleyite at 800 °C, 12 kbar, by a sensitive weight-change method. Dissolution occurs incongruently according to the reaction:

$$ZrSiO_4 = ZrO_2 + SiO_{2(t)}$$
zircon   baddeleyite
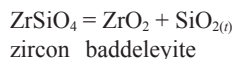
where $SiO_{2(t)}$ is total dissolved silica. Blank runs demonstrated that the effects of ZrO_2 solubility and/or capsule-Pt transfer were near the weighing detection limit, so weight losses or gains could be ascribed quantitatively to SiO_2 solubility. Precise $SiO_{2(t)}$ concentrations were ensured by use of three types of starting material, by approaching equilibrium from zircon-undersaturation and oversaturation, and by demonstrating time-independence of the measurements. The results yielded a SiO_2 concentration of 0.069 ± 0.002 (1 se) moles per kg H_2O (m_s), or a mole fraction (X_s) of $1.23 \times 10^{-3} \pm 3.3 \times 10^{-5}$. Two runs on zircon solubility in $NaCl$-H_2O solutions at 800 °C and 10 kbar showed silica solubility to decrease by nearly 1% per mol% NaCl.

The standard molar Gibbs free energy of formation of zircon from the oxides at a constant P and T is given by:

$$\Delta G^{\circ}_{f,ox,zr} = RT \ln \frac{\gamma_s^{ZB} X_s^{ZB}}{\gamma_s^{Q} X_s^{Q}}$$

where ZB and Q refer, respectively, to equilibrium with zircon-baddeleyite and quartz, γ_s is the activity coefficient of total silica, and the relationship between γ_s and X_s accounts for aqueous silica activity. Our results yield $\Delta G^{\circ}_{f,ox,zr} = -18.5 \pm 0.7$ kJ/mol at 800 °C, 12 kbar (95% confidence), or a standard apparent Gibbs free energy of formation from the elements of -1918.3 ± 0.7 kJ/mol at 25 °C, 1 bar. Our value is consistent with determinations based on phase equilibrium studies, within reported error limits, but is more precise than most previous values. However, it is less negative than high-temperature determinations by calorimetry and electrochemistry. Our results indicate that solubility measurements at high T and P may be a superior method of free energy determination of other refractory silicate minerals.

Keywords: Experimental petrology, phase equilibria, thermodynamics, zircon

INTRODUCTION

Zircon, $ZrSiO_4$, is one of the most important minerals for geochronology (Davis et al. 2003) and for tracing geologic processes (e.g., Hoskin and Schaltegger 2003; Hanchar and Watson 2003). In addition to its ability to incorporate U and Th and exclude non-radiogenic Pb, it possesses great thermodynamic stability. This stability is manifest in its low solubility in aqueous fluids and magmas, and in its compatibility with most common rock-forming mineral assemblages over large ranges of pressure (P) and temperature (T). Zircon saturation in H_2O-bearing granite melts near liquidus temperatures occurs at Zr contents of only about 100 ppm (Harrison and Watson 1983), which virtually guarantees that it is a common liquidus mineral. In addition, low diffusion rates in zircon enable retention of radioactive and daughter isotopes as well as other constituent elements (Cherniak and Watson 2003), which lead to zircon's utility in geothermometry (e.g., Watson and Harrison 2005; Watson et al. 2006; Ferry and Watson 2007). Finally, the refractory character of zircon promotes survival through dynamothermal events subsequent to crystallization. These factors conspire to make zircon a common phase in many igneous, metamorphic, and sedimentary lithologies.

The great stability of zircon has hampered attempts to define its fundamental thermodynamic properties. Insolubility in acids

* E-mail: manning@ess.ucla.edu

or other aqueous fluids at low P and T renders conventional solution calorimetry ineffective. A paucity of reversible reactions with other refractory substances at elevated P-T conditions accounts for exclusion of zircon from earlier self-consistent data sets of thermodynamic properties based primarily on experimental phase equilibrium.

The first experimental determination of the Gibbs free energy of formation of zircon from its oxides, $\Delta G^{\circ}_{f,ox,zr}$, was performed by Rosén and Muan (1965). They measured the CO/CO_2 ratios of gases equilibrated with zircon, ZrO_2, $CoSiO_4$, Co metal, and SiO_2 at 1 bar and 1180–1366 °C. Solid-vapor equilibrium was established for two reactions:

$$ZrO_2 + Co_2SiO_4 + 2\ CO = ZrSiO_4 + 2\ Co + 2\ CO_2 \qquad (1)$$
$$Co_2SiO_4 + 2\ CO = 2\ Co + SiO_2 + 2\ CO_2. \qquad (2)$$
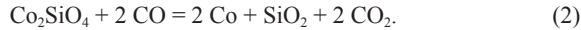
The actual ZrO_2 and SiO_2 phases encountered in this study were the high-T tetragonal form and cristobalite, respectively. When reactions 1 and 2 are combined, and allowance is made for phase changes in ZrO_2 and SiO_2, the data yield zircon formation from its oxides:

$$ZrO_2\ +\ SiO_2 = ZrSiO_4. \qquad (3)$$
$$\text{baddeleyite} \quad \text{quartz} \quad \text{zircon}$$
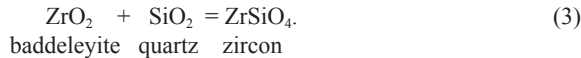
The equilibrium constant of the zircon-forming reaction involves only the CO/CO_2 ratios of the two redox reactions. Though the ratios were measured precisely, the limited temperature range of the Rosén and Muan (1965) observations yields unreliable extrapolation to lower temperatures, as the T dependence of the equilibrium constant is inconsistent with that derived from calorimetric study (Ellison and Navrotsky 1992).

Schuiling et al. (1976) constrained $\Delta G^{\circ}_{f,ox,zr}$ by investigating monotropic reactions of zircon with other minerals in SiO_2-undersaturated systems at 1000 K and 1 kbar. They bracketed the SiO_2 activity buffered by zircon + baddeleyite based on the SiO_2 activities defined by several equilibria involving zircon and minerals whose free energies of formation were reasonably well known. Their derived $\Delta G^{\circ}_{f,ox,zr}$ was only constrained broadly within a range of 7.8 kJ/mol, exclusive of uncertainties in ΔG°_{f} of the other minerals in the reactions.

Ellison and Navrotsky (1992) measured the enthalpies of solution of zircon, baddeleyite, and quartz at 977 K in $Pb_2B_2O_5$ melt; this was the first successful enthalpy of formation measurement on zircon. This measurement, in conjunction with existing low-temperature heat capacity and high-temperature heat content data for the phases, provided $\Delta G^{\circ}_{f,ox,zr}$ values over a large T range. Though Ellison and Navrotsky (1992) identified the general range of zircon enthalpy and free energy, the relatively low precision of the high-T solution calorimetry method yields large uncertainties (Table 1).

Thermodynamic properties for zircon tabulated in the major data sets draw from the above sources and are subject to the largest uncertainties for any orthosilicate in the tables. Holland and Powell (1998) cite the zircon free energy data given in the compendium of Robie et al. (1979), which, in turn, cites Schuiling et al. (1976), though the values given in these sources are greatly disparate. The Berman (1988) value is close to that of

TABLE 1. Summary of data for zircon ΔG°_{f} at 1 bar

$\Delta G^{\circ}_{f,elements}$ at 298 K (kJ/mol)	$\Delta G^{\circ}_{f,oxides}$ at 1073 K (kJ/mol)	Uncertainty type	Source
−1919.3 ± 2.3	−12.9 ± 2.3	1	Rosén and Muan (1965)*
−1923.3 ± 3.9	−17.0 ± 3.9	1	Schuiling et al. (1976)
−1917.4	−11.1	0	Berman (1988)
−1922.9 ± 3.7	−16.5 ± 3.7	2	Ellison and Navrotsky (1992)
−1919.7	−13.4	0	Robie and Hemingway (1995)
−1917.3 ± 3.4	−11.0 ± 3.4	2	Holland and Powell (1998)
−1918.5 ± 1.5	−12.2 ± 1.5	1	Ferry et al. (2002), consistent with Holland and Powell (1998)
−1917.5 ± 1.3	−11.2 ± 1.3	1	Ferry et al. (2002), consistent with Berman (1988)
−1918.5 ± 1.2	−12.1 ± 1.2	2	Newton et al. (2005)
−1920.9 ± 0.4	−14.5 ± 0.4	2	O'Neill (2006)
−1918.3 ± 0.7	−11.9 ± 0.7	2	Present study

Note: High-T experimental values from listed sources were combined with Robie and Hemingway (1995) heat capacities and oxide data to calculate 298 and 1073 K data and high-P data recalculated at 1 bar using compressibilities in Holland and Powell (1998) (errors in these data are neglected as they are shared); values may therefore differ from those reported in original source. Uncertainty types: 0, no error reported; 1, one half the range between minimum and maximum constraints; 2, 95% confidence interval.
* Average of values between 1453–1639 K.

Holland and Powell (1998), but suffers from the same limitations in source data, though uncertainties are not reported. The tables of Robie and Hemingway (1995) give yet a different value for zircon free energy of formation (Table 1).

Ferry et al. (2002) determined three reversed brackets of the univariant equilibrium:

$$ZrSiO_4 + 2\ MgCO_3 = Mg_2SiO_4 +\ ZrO_2\ + 2\ CO_2 \qquad (4)$$
$$\text{zircon} \quad \text{magnesite} \quad \text{forsterite} \quad \text{baddeleyite}$$
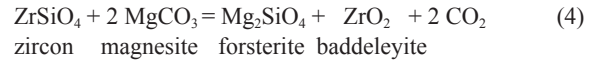
at 800–900 °C, 7–12 kbar. These are the only existing reversed phase equilibrium data of sufficient precision to define the free energy of zircon relative to other substances with measured thermodynamic properties. However, the tabulated free energy data of the minerals of reaction 4 differ substantially between the major data sets. Moreover, the free energy data for CO_2 given by Mäder and Berman (1991) and Holland and Powell (1998) data sets differ by about 2 kJ/mol in this P-T range. For these reasons, the derived free energy of formation in Table 1 differs by 1 kJ depending on the data set used to supply thermodynamic data for participating phases.

Newton et al. (2005) showed that the concentration of silica in H_2O in equilibrium with the zircon + baddeleyite buffer:

$$ZrSiO_4 =\ ZrO_2 + SiO_{2(t)} \qquad (5)$$
$$\text{zircon} \quad \text{baddeleyite}$$

at high P and T could be used to constrain thermodynamic properties of zircon. Synthetic zircon single crystals were altered to baddeleyite in tightly adhering surface coatings after 2–4 days at 800 °C, 12 kbar. Weight losses gave apparent $SiO_{2(t)}$ molality of about 0.07 under the interpretation of reaction 5. These data, in conjunction with an activity-concentration model for aqueous silica (Newton and Manning 2003), yielded a value for zircon free energy of formation that is independent of previous assessments and more precise than most (Table 1). However, this study lacked rigorous blank testing and used a limited set of materials to measure solubility.

The most precise determination of the free energy of forma-

tion of zircon is that of O'Neill (2006), in an electrochemical cell using the zirconia solid electrolyte at 1100–1300 K. Oxygen potentials of two assemblages—fayalite-iron-quartz and fayalite-iron-baddeleyite-zircon—were measured; their difference, at a given temperature, gives a free energy change of reaction 3 that is more negative than most phase-equilibrium determinations (Table 1). In spite of the high precision of the determination of O'Neill (2006) (±0.4 kJ, 2σ), the results cannot be considered definitive for several reasons, including the fact that the temperature coefficient of the free energy of formation of fayalite differs considerably from the previous determination of O'Neill (1987), which was used to calculate the zircon free energy. Also, the thermophysical properties and monoclinic-to-tetragonal inversion temperature of baddeleyite preferred by O'Neill (2006) differ substantially from those recently reported by Moriya and Navrotsky (2006).

In view of the continuing disagreement in the thermodynamic properties of zircon, the present study built on Newton et al. (2005) in an attempt to improve accuracy and precision of the silica concentration in equilibrium with zircon, baddeleyite, and H_2O (reaction 5) at 800 °C and 12 kbar, which would then yield an improved value for $\Delta G^\circ_{f,ox,zr}$ (reaction 3). A variety of starting materials in different states of aggregation were used, and emphasis was placed on demonstration of reversibility and time-independence of measurements, as well as narrowly defined brackets. Several solubility measurements were also made on ZrO_2 (baddeleyite) in H_2O, and on zircon and baddeleyite in moderately concentrated NaCl solutions, to explore the possible effects of any solute species other than silica.

EXPERIMENTAL METHODS

Three kinds of starting materials were used (Table 2). Ten experiments, seven of which are from Newton et al. (2005), employed euhedral, synthetic, flux-grown zircon crystals (~0.5 mm; Hanchar et al. 2001). The crystals were optically flawless and contained no visible flux inclusions. A second type of starting material, used in five runs (Table 2), was a fine-grained polycrystalline mixture of zircon and

baddeleyite of subequal mass, synthesized hydrothermally at 900 °C and 12 kbar for 48 h from a baked (900 °C, 20 min) mixture of ZrO_2 reagent (Matheson) plus ultrapure SiO_2 (Aesar). The ZrO_2 contained a maximum of 2 wt% Hf as the only significant impurity. The synthesis yielded equant crystals of zircon up to 80 μm diameter. The baddeleyite was recrystallized but finer-grained (~5 μm). Tetragonal unit-cell constants of the zircon were determined by powder X-ray diffraction scans (Cu$K\alpha_1$, 1 °2θ/min), using the baddeleyite peaks (ASTM file 36-420) as an internal standard. The values of $a_o = 6.600(1)$ and $c_o = 5.975(2)$ (1σ) are in exact agreement with those given in ASTM file 6-0266. The third kind of starting material was a sintered pellet of the Matheson ZrO_2 (four experiments; Table 2). Reagent ZrO_2 was pelletized under pressure and heated in air at 1100 °C for 2 h—close to, but below the upper stability limit of baddeleyite relative to high-T, tetragonal ZrO_2. Chips of the pellet weighing 2 to 7 mg were rounded into small ellipsoids with a file and smoothed with 600-mesh Al_2O_3 paper prior to use.

In each experiment, the starting material was encased in an inner capsule formed from a 3 mm long, 1.5 mm O.D. Pt tube that was lightly crimped at the ends and perforated with small pinholes to allow access of fluids. Inner capsules were necessary to confine granular starting materials and reaction products. Tubes and solid materials were heated in air at 400 °C for 10–15 min prior to weighing in, to purge any volatiles. The inner capsule was then placed in a ~1.6 cm long, 3 mm O.D. Pt capsule with 0.02 mm wall thickness, with ~33 mg distilled and deionized H_2O. In most runs, a small natural quartz chip (Newton and Manning 2000) was also weighed into the outer capsule. Because the quartz dissolves very rapidly at high P and T, it is assumed that this approach set the initial silica concentration above or below the final value prior to significant zircon reaction, permitting approach to equilibrium from over- or undersaturation.

Experiments were conducted in a ¾ inch diameter piston-cylinder apparatus with NaCl pressure medium and graphite heater sleeve. Temperatures were measured and controlled with W3%Rh-W25%Rh thermocouples. Pressure and temperature uncertainties are ±300 bars and ±3 °C.

Runs were terminated by quenching to below 200 °C in <12 s. Retrieved and cleaned capsules weighed within 0.03% of starting values. H_2O contents were checked by puncturing and drying the capsules at 115 °C for 15 min followed by 320 °C for 15 min, taking care to retain all of the solid residue. The H_2O determined this way was within 0.6% of the initial values. The outer capsules were cut open with a razor blade, taking care not to score the inner capsule. Interiors of the outer capsules were examined for vapor-transport or escaped crystals (Caciagli and Manning 2003; Tropper and Manning 2005). Two experiments in which they were found were discarded. In all of the other experiments, only a dried residue was present in the outer capsules. This thin coating of translucent siliceous gel was interpreted as quench from the fluid phase. Contents of the inner capsules were retrieved after weighing and examined in immersion oils with the optical microscope, by scanning electron microscopy, and in some cases by X-ray diffraction, to confirm the

TABLE 2. Experimental results, 800 °C, 12 kbar

Expt. no.	Starting material*	Time (h)	wt Qtz in (mg)	wt inner capsule in (mg)	wt inner capsule out (mg)	wt H_2O (mg)	m_{SiO_2}† (mol/kg ±0.002)	$10^3 X_{SiO_2}$† (±0.04)	Reaction direction‡
ZR-2	F-ZB	110		65.723	65.609	32.282	0.057	1.02	↑
ZR-3	F-ZBQ	115	0.187	71.992	72.058	32.118	0.061	1.09	↓
ZR-4	S-Z	109		70.303	70.185	32.967	0.058	1.04	↑
ZR-6	F-ZBQ	92	0.229	74.819	74.887	32.546	0.080	1.44	↓
ZR-8	F-ZBQ	116	0.131	73.749	73.744	33.154	0.066	1.19	↑
ZR-9	P-BQ	100	0.311	83.709	83.874	33.183	0.071	1.28	↓
ZR-10	F-ZBQ	116	0.208	74.020	74.078	33.166	0.073	1.32	↓
ZR-11	S-(ZB)Q	110	0.172	66.027	66.065	32.676	0.066	1.19	↓
ZR-12	S-Z	112		68.030	67.899	32.877	0.064	1.16	↑
ZR-13	P-BQ	112	0.264	79.934	80.035	33.465	0.079	1.42	↓
ZR-14	S-(ZB)Q	112	0.188	69.154	69.196	33.157	0.071	1.28	↓
ZR-16	P-BQ	96	0.339	67.490	67.683	31.539	0.075	1.35	↓
ZR-17	S-ZQ	88	0.085	66.533	66.483	32.775	0.067	1.20	↑
ZR-18	S-Z	70		66.432	66.289	34.056	0.068	1.22	↑
ZR-20	S-ZQ	72	0.042	2.605§	2.500§	32.768	0.073	1.31	↑
ZR-21	P-BQ	61	0.403	75.704	75.900	34.540	0.098	1.76	↓
ZRS-3	S-Z	5		74.448	74.283	37.913	0.071	1.27	↑
ZRS-1‖	S-Z	24		80.069	79.948	33.537	0.058	1.04	↑
ZRS-2‖	S-Z	20		74.195	74.108	26.553	0.052	0.94	↑

* Abbreviations: S = single crystal; F = fine-grained synthetic crystals; P = sintered pellet; B = baddeleyite; Q = quartz (single crystal, in outer capsule); Z = zircon; ZB = zircon crystal coated with fine-grained baddeleyite
† m_{SiO_2} and X_{SiO_2} corrected for 0.004 mg ZrO_2 solubility and/or Pt loss (Table 3, see text). Uncertainty is 1σ, from propagated 1σ = 2 μg error in all weights.
‡ Downward-pointing and upward-pointing arrows denote equilibrium approached from high and low concentration, respectively.
§ Weight of zircon crystal; no inner capsule used.
‖ Experiments with added NaCl. NaCl mole fraction was 0.103 in ZRS-1 and 0.198 in ZRS-2.

reaction direction as indicated by the weight changes.

Several experiments were made to determine weight losses from ZrO_2 and/or Pt dissolution (Table 3). Most of these experiments were made with the sintered pellet material without quartz. Two experiments with quartz, but undersaturated with respect to zircon, were made to calibrate the effect of the small amount of quenched and dried siliceous vapor precipitate in the inner capsule.

Two experiments on zircon and one on baddeleyite were conducted with added NaCl (Tables 2 and 3). NaCl was first loaded into the outer capsule a solid reagent, and then H_2O was added so as to achieve a desired NaCl mole fraction. These runs tested for possible ZrO_2 or $ZrSiO_4$ solubility enhancements similar to that found in Al_2O_3 (Newton and Manning 2006, 2008).

Weights were determined with a Mettler M3 microbalance ($1\sigma = 2$ μg). Several blank experiments utilized a higher precision ultramicrobalance, for which $1\sigma = 0.2$ μg. Concentration uncertainties in Table 2 are solely due to propagated weighing errors.

RESULTS

Experimental data are given in Tables 2 and 3. Weight losses of the inner capsules were interpreted as SiO_2 loss via baddeleyite growth during incongruent dissolution of zircon; these runs approached equilibrium SiO_2 fluid concentration from the undersaturated direction. Nucleation and growth of baddeleyite was confirmed for the single-crystal experiments by SEM images, which showed tightly adhering fine-grained baddeleyite coating the zircons, with preservation of the zircon crystal morphology (Newton et al. 2005). Nucleation and growth of zircon in the reversal experiments, indicated by weight gains of the inner Pt capsules, was confirmed by SEM images of the sintered ZrO_2 pellets. Figure 1 shows large, flat zircon crystals that nucleated and grew on the surface of a sintered ZrO_2 pellet in one experiment (ZR-9) in which the initial SiO_2 content of the fluid (0.16 m) substantially exceeded the final concentration (0.07 m), as indicated by the weight gain. Minor coarsening of baddeleyite grains of the substrate is also evident.

Blank runs (Table 3) indicate an average weight loss of 0.004 mg, from ZrO_2 solubility and/or Pt transfer from the inner capsule. These marginally significant effects could not be separated; they may be merely the result of "steam cleaning" of the Pt. In any case, the small amount of ZrO_2 in the fluid phase from zircon dissolution does not contribute significantly to the total weight change, which can therefore be ascribed to SiO_2. Thus, after incorporation of a blank correction of –0.004 mg into results, the remaining weight change was used to compute the final SiO_2 concentrations of Table 2.

Results of experiments show no systematic differences between the three kinds of starting material. Figure 2a indicates that runs approaching equilibrium from undersaturation yield a similar solubility independent of run duration, even in the case of the 5 h experiment (ZRS-3). By contrast, runs in which Si concentration was initially supersaturated appear to take longer to equilibrate: run ZR-21 (61 h) appears to be underequilibrated relative to longer experiments, although its initial SiO_2 concentration was also furthest from the final value (Table 2). Slight crossovers of the mean SiO_2 concentration occurred from opposite directions, in experiments ZR-20 (flux-grown crystals) and ZR-3 (fine-grained crystal mixture).

Figure 2a thus demonstrates that the experiments yielded a constant solution concentration that is independent of starting material, direction of reaction, and run duration, for runs ≥70 h. Figure 2b demonstrates that the inferred equilibrium SiO_2 concentration is independent of the initial SiO_2 fluid concentration

TABLE 3. Blank experiments on ZrO_2 and empty capsules, 800 °C, 12 kbar

Expt. no.	Starting material	Time (h)	wt inner capsule in (mg)	wt inner capsule out (mg)	wt quartz (mg)	wt H_2O (mg)	Δic no. (mg)
2	none	5	78.390	78.386	0	33.069	–0.004
3	none	24	72.137	72.134	0	32.956	–0.003
ZrO_2-6	P-B	24	76.198	76.190	0	33.337	–0.008
ZrO_2-2	P-B	69	76.685	79.681	0	36.256	–0.004
ZR-19	P-B	70	60.945	60.942	0	32.366	–0.003
ZR-15	P-B	72	65.311	65.307	0	32.452	–0.004
ZrO_2-1*	P-B	48	48.958	48.958	0	23.704*	–0.000
ZR-24	P-BQ	20	65.9866	65.9848	0.0701	37.599	–0.0018
ZR-25	P-BQ	20	68.8402	68.8390	0.1542	38.554	–0.0012

Notes: See Table 2 for abbreviations. Weights reported to three decimal places were determined on a Mettler M3 microbalance ($1\sigma = 2$ μg), whereas those reported to four places were determined on a Mettler UMX2 ultramicrobalance ($1\sigma = 0.2$ μg).
* NaCl mole fraction was 0.214.

FIGURE 1. (**a**) Backscattered electron image of sintered ZrO_2 pellet from experiment ZR-9 (Table 2), showing spontaneously nucleated large zircon crystals grown from small initial SiO_2 oversaturation at 800 °C and 12 kbar. Region in white box enlarged in **b**.
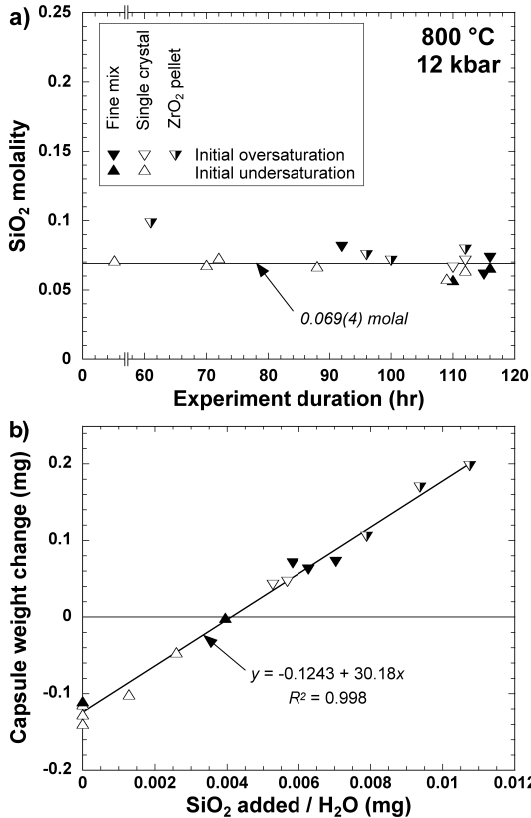
FIGURE 2. (a) SiO$_2$ molality at zircon + baddeleyite at 800 °C and 12 kbar, as a function of experiment duration. Symbols show results from three different kinds of starting materials (see text). Triangle apices point in the direction of approach to equilibrium, both from undersaturated and oversaturated directions. **(b)** Capsule weight change vs. SiO$_2$ added to experiment (as powdered quartz crystals) per milligram of H$_2$O. Experiments ZR-21 and ZRS-3 omitted (see text). Regression of weight-change data constrains the best value of SiO$_2$ solubility of zircon. The SiO$_2$/H$_2$O value at the null point of the ordinate gives, when multiplied by 1000/60.084, the equilibrium SiO$_2$ molality.

because no systematic departures from a linear regression of the data are evident (<70 h runs omitted). Experiments of ≥70 h duration are therefore interpreted to be equilibrated. The average solubility obtained from the 15 equilibrated experiments is 0.0686 ± 0.0071 m (1σ), corresponding to a SiO$_2$ mole fraction of 0.00123 ± 0.00013. Standard errors in mean molality and mole fraction are 0.0018 and 0.000033, respectively.

The data on zircon solubility in H$_2$O-NaCl solutions (Table 2) indicate that a 20% reduction in H$_2$O mole fraction at 800 °C and 12 kbar results in nearly a 20% reduction in silica molality. The solubility of ZrO$_2$ was not enhanced by NaCl or SiO$_2$ (Table 3).

DISCUSSION

The new determination of aqueous SiO$_2$ concentration in equilibrium with zircon + baddeleyite may be used with our measurements of quartz solubility (Newton and Manning 2003) to derive an accurate value of $\Delta G^\circ_{f,ox,zr}$ (e.g., Hemley et al. 1977). In this derivation, it is necessary to know precisely the activity coefficient of aqueous silica at zircon saturation and at quartz

saturation, because aqueous SiO$_2$ undergoes changes in polymerization extent that depend on P, T, and composition (Zotov and Keppler 2000, 2002; Zhang and Frantz 2000; Newton and Manning 2002, 2003, 2008). At 800 °C and 12 kbar, aqueous SiO$_2$ consists almost entirely of monomers and dimers, for which homogeneous equilibrium can be written as

$$2\ SiO_{2(m)} = Si_2O_{4(d)}. \tag{6}$$
monomer dimer

Assuming ideal mixing, the equilibrium constant for this reaction is $K_{md} = X_d/X_m^2$, where X_d and X_m are mole fractions of dimers and monomers. Mass balance requires that $X_s = X_m + 2X_d$, where X_s is the mole fraction of total SiO$_2$. Taking the standard state of solute silica to be unit activity in the hypothetical solution of pure SiO$_2$ monomers at fixed P and T, the equilibrium constant for Equation 6 is

$$K_{md} = \frac{(1-\gamma_s)}{2\gamma_s^2 X_s} \tag{7}$$

where γ_s is the activity coefficient of solute silica.

Newton and Manning (2003) determined the activity coefficient of aqueous silica at 800 °C and 12 kbar from low concentration to quartz saturation from the SiO$_2$ solubilities of four silica-buffering mineral assemblages:

Q:	$SiO_2 = SiO_{2(t)}$	(8)
	quartz	
KC:	$Al_2SiO_5 = Al_2O_3 + SiO_{2(t)}$	(9)
	kyanite corundum	
EF:	$MgSiO_3 = Mg_2SiO_4 + SiO_{2(t)}$	(10)
	enstatite forsterite	
FRG:	$2\ TiO_2 + Mg_2SiO_4 = 2\ MgTiO_3 + SiO_{2(t)}$	(11)
	rutile forsterite geikielite	
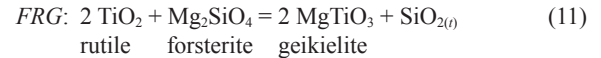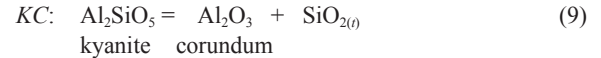
Combination of the quartz buffer (Q, reaction 8) with any of the other silica buffers generates the relationship

$$\Delta G^\circ_{B-Q} = -RT \ln \frac{\gamma_s^B X_s^B}{\gamma_s^Q X_s^Q} \tag{12}$$

where B represents a silica buffer [reactants = products + SiO$_{2(t)}$], and ΔG°_{B-Q} is the difference in standard molal Gibbs free energy changes of reactions B and Q at a fixed P and T. Standard states for minerals and H$_2$O are unit activity of the pure phase at any P and T. Given reliable ΔG°_{B-Q} values, the experimental solubility data for reactions 8–11 can be fitted to give $\gamma_s = f(X_s)$ (Newton and Manning 2003).

Newton and Manning (2003) found that their solubility measurements corresponding to reactions 8–11 calibrate a monomer-dimer activity model with high fidelity, resulting in K_{md} of 116–180 at 800 °C and 12 kbar, using mineral data of Holland and Powell (1998). Because there is equal probability of any value between the upper and lower bounds, we here adopt $K_{md} = 148$ with σ = $(K_{md}^{max} - K_{md}^{min})/\sqrt{12} = 18.5$. With this value, the activity coefficient for a concentration of $X_s = 0.00123 \pm 0.000033$ (1 se), corresponding to zircon saturation, is 0.779 ± 0.018 (1σ). Thus, the solute silica at 800 °C and 12 kbar is

substantially polymerized (22%) even at the dilute concentration of zircon saturation. At quartz saturation, $X_s = 0.0248 \pm 0.00028$ (Newton and Manning 2003), $\gamma_s = 0.307 \pm 0.016$, and the solution is ~70% polymerized.

The free energy of formation of zircon from the oxides at 800 °C and 12 kbar can be calculated from a version of Equation 12 written explicitly for the zircon-baddeleyite silica buffer:

$$\Delta G^\circ_{f,ox,zr} = \Delta G^\circ_{ZB-Q} = RT \ln\left(\frac{\gamma_s^{ZB} X_s^{ZB}}{\gamma_s^{Q} X_s^{Q}}\right) \qquad (13)$$

which yields −18.5 kJ/mol. Uncertainties were estimated numerically (10 000 trials) using the following errors: $K_{md} = 18.5$; $X_s^{ZB} = 3.3 \times 10^{-5}$; and $X_s^{Q} = 2.8 \times 10^{-4}$. This gave $1\sigma = 0.33$ kJ/mol, or a 95% confidence interval of 0.65 kJ/mol. Our value for $\Delta G^\circ_{f,ox,zr}$ at 800 °C and 12 kbar was referred to 1 bar and 800 °C using the compressibility coefficients for zircon, baddeleyite, and quartz of Holland and Powell (1998) to obtain $\Delta G^\circ_{f,ox,zr}$ at 1073 K of −11.9 ± 0.7 kJ/mol (errors in compressibilities neglected). This in turn leads to the free energy of formation of zircon from the elements, $\Delta G^\circ_{f,el,zr}$, at 25 °C, 1 bar, of −1918.3 ± 0.7 kJ/mol, using heat capacity and oxide data from Robie and Hemingway (1995).

The results of the present study are compared with those of previous studies in Table 1 and Figure 3. The new constraints are virtually identical to those of Newton et al. (2005) and Ferry et al. (2002), but with higher precision afforded by the large number of measurements constraining X_s^{ZB}. Agreement among results obtained using different starting materials gives confidence in the accuracy of the data.

The result also agrees well with the data of Rosén and Muan (1965), but only through use of independently derived functions for the dependence of Gibbs energy on T (Robie and Hemingway 1995). This is because the T interval over which their data were collected was too narrow, leading to an inaccurate temperature coefficient of zircon free energy of formation in their study. With this adjustment, and by assuming that their polythermal data can be treated as a single constraint at their median T (with corresponding uncertainties), the Rosén and Muan (1965) result is in very good agreement with the more recent determinations (Table 1; Fig. 3). In contrast, the data of Schuiling et al. (1976) are more negative than other phase equilibrium studies. It is notable that uncertainty in their constraint is the largest of any study—and may be considerably underestimated because it does not account for errors in thermochemical data for the other substances involved in the bracketing reactions.

The values for the free energy of formation of zircon derived from high-temperature solution calorimetry (Ellison and Navrotsky 1992) and electrochemical methods (O'Neill 2006) are more negative than those derived from phase equilibrium approaches. The former result, which was recalculated using heat capacity functions of Robie and Hemingway (1995) for consistency, is beyond the 95% confidence limits of the present determination, even when their >5× larger uncertainties are taken into account. The O'Neill (2006) value is 2.6 kJ/mol more negative than the present determination. Though the difference in energy is not large, the high precision of both determinations
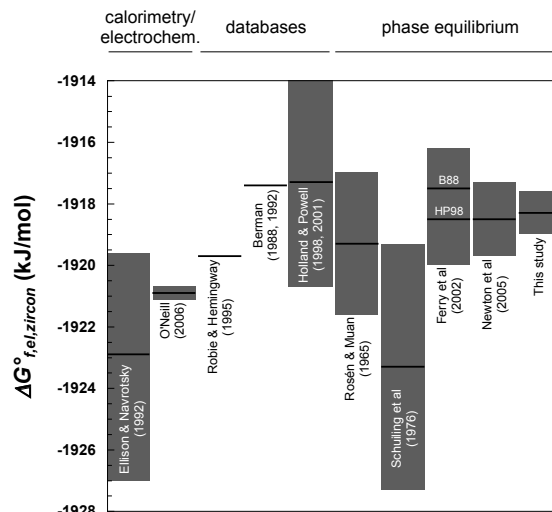
FIGURE 3. Comparison of determinations of $\Delta G^\circ_{f,el,zircon}$, at 25 °C and 1 bar from different sources and methods. Uncertainties are given at the 95% confidence level or full range of bracketing constraints (Table 1). The determinations from phase equilibrium studies, including the present work, are in good agreement. In contrast, the determination by solution calorimetry (Ellison and Navrotsky 1992) and the electrochemical determination (O'Neill 2006) differ from this study.

implies that the two studies differ at a statistically significant level. A more fundamental critique of the various techniques will be needed to resolve this discrepancy.

The Holland and Powell (1998) and Berman (1992) data sets give values of $\Delta G^\circ_{f,ox,zr}$ at 800 °C that are in apparent agreement with each other (Table 1). It may be shown, however, that the zircon data and the free energy change of geikielite + quartz to rutile + forsterite given in both data sets are incompatible with the experimental work of Ferry et al. (2002) on reaction 4 and

$$TiO_2 + MgCO_3 = MgTiO_3 + CO_2. \qquad (14)$$
rutile magnesite geikielite
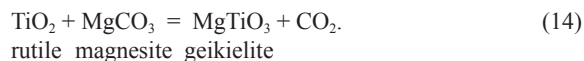
The fact that the equilibrium pressure of reaction 4 (7.6 kbar at 800 °C) is higher than that of reaction 14 (7.05 kbar at 800 °C) logically requires that $\Delta G^\circ_{f,ox,zr} = \Delta G^\circ_{ZB-Q} < \Delta G^\circ_{FRG-Q}$. This expectation is fulfilled in the present work: our value of −18.5 kJ for ΔG°_{ZB-Q} is more negative than the −17.4 kJ for ΔG°_{FRG-Q} adopted by Newton and Manning (2003).

In summary, we have demonstrated that high P-T solubility methods can be used to obtain the free energy of formation of zircon, a refractory substance that has proven challenging to characterize accurately by more conventional methods of investigation. Our result is compatible with most of the previous determinations based on phase equilibrium analysis, but is more precise than any. We find good agreement with the high-T redox gas-reaction study of Rosén and Muan (1965), when their data are referred to lower temperatures by independently measured thermophysical data. Our data are also in good agreement with the study of Ferry et al. (2002). Our precision is at least five times better than earlier measurements based on high-temperature solution calorimetry

and free energy bracketing by monotropic reactions.

The present methods may be of value in defining the thermodynamic properties of other refractory silicates where SiO_2 is the dominant solute. These may include aluminum silicates, cordierite, titanite, sapphirine, and Mg-Al and Ca-Al garnets. The precision obtainable by our methods suggests that studies of the free energy of Si-Al order-disorder and solid solution may be feasible in some mineral systems. It may be also possible to characterize the energetics of radioactivity damage in metamict zircons, which would have applications to radiometric age-dating methods.

ACKNOWLEDGMENTS

REFERENCES CITED

Berman, R.G. (1988) Internally-consistent thermodynamic data for minerals in the system Na₂O-K₂O-CaO-MgO-FeO-Fe₂O₃-Al₂O₃-SiO₂-TiO₂-H₂O-CO₂. Journal of Petrology, 29, 445–522.

Caciagli, N.C. and Manning, C.E. (2003) The solubility of calcite in water at 5–16 kbar and 500–800 °C. Contributions to Mineralogy and Petrology, 146, 275–285.

Cherniak, D.J. and Watson, E.B. (2003) Diffusion in zircon. In J.M. Hanchar and P.W.O. Hoskin, Eds., Zircon, 53, p. 113–143. Reviews in Mineralogy and Geochemistry, Mineralogical Society of America, Chantilly, Virginia..

Davis, D.W., Williams, I.S., and Krogh, T.E. (2003) Historical development of zircon geochronology. In J.M. Hanchar and P.W.O. Hoskin, Eds., Zircon, 53, p. 145–181. Reviews in Mineralogy and Geochemistry, Mineralogical Society of America, Chantilly, Virginia.

Ellison, A.J.G. and Navrotsky, A. (1992) Enthalpy of formation of zircon. Journal of the American Ceramic Society, 75, 1430–1433.

Ferry, J.M. and Watson, E.B. (2007) New thermodynamic models and revised calibrations for the Ti-in-zircon and Zr-in-rutile thermometers. Contributions to Mineralogy and Petrology, 154, 429–437.

Ferry, J.M., Newton, R.C., and Manning, C.E. (2002) Experimental determination of the equilibria: rutile + magnesite = geikielite + CO₂ and zircon + 2 magnesite = baddeleyite + 2 CO₂. American Mineralogist, 87, 1342–1350.

Hanchar, J.M. and Watson, E.B. (2003) Zircon saturation thermometry. In J.M. Hanchar and P.W.O. Hoskin, Eds., Zircon, 53, p. 89–112. Reviews in Mineralogy and Geochemistry, Mineralogical Society of America, Chantilly, Virginia.

Hanchar, J.M., Finch, R.J., Hoskin, P.W.O., Watson, E.B., Cherniak, D.J., and Mariano, A.N. (2001) Rare earth elements in synthetic zircon. 1. Synthesis and rare earth element and phosphorus doping. American Mineralogist, 86, 667–680.

Harrison T.M. and Watson, E.B. (1983) Kinetics of zircon dissolution and zirconium diffusion in granitic melts of variable water content. Contributions to Mineralogy and Petrology, 84, 66–72.

Hemley, J.J., Montoya, J.W., Shaw, D.R., and Luce, R.W. (1977) Mineral equilibria in the MgO-SiO₂-H₂O system: II Talc-antigorite-anthophyllite-enstatite stability relations and some geological implications in the system. American Journal of Science, 277, 322–351.

Holland, T.J.B. and Powell, R. (1998) An internally consistent data set for phases of petrologic interest. Journal of Metamorphic Geology, 16, 309–343.

Hoskin, P.W.O. and Schaltegger, U. (2003) The composition of zircon and igneous and metamorphic petrogenesis. In J.M. Hanchar and P.W.O. Hoskin, Eds., Zircon, 53, p. 27–62. Reviews in Mineralogy and Geochemistry, Mineralogical Society of America, Chantilly, Virginia.

Mäder, U.K. and Berman, R.G. (1991) An equation of state for carbon dioxide to high pressure and temperature. American Mineralogist, 76, 1547–1559.

Moriya, Y. and Navrotsky, A. (2006) High-temperature calorimetry of zirconia: heat capacity and thermodynamics of the monoclinic-tetragonal phase transition. Journal of Chemical Thermodynamics, 38, 211–223.

Newton, R.C. and Manning, C.E. (2000) Quartz solubility in H₂O-NaCl and H₂O-CO₂ at deep crust-upper mantle pressures and temperatures: 2–15 kbar and 500–900 °C. Geochimica et Cosmochimica Acta, 64, 2993–3005.

――― (2002) Solubility of enstatite + forsterite in H₂O at deep crust/upper mantle conditions: 4–15 kbar and 700–900 °C. Geochimica et Cosmochimica Acta, 66, 4165–4176.

――― (2003) Activity coefficient and polymerization of aqueous silica at 800 °C, 12 kbar, from solubility measurements on SiO₂-buffering mineral assemblages. Contributions to Mineralogy and Petrology, 146, 135–143.

――― (2006) Solubilities of corundum, wollastonite and quartz in H₂O-NaCl solutions at 800 °C and 10 kbar: Interactions of simple minerals with brines at high pressure and temperature. Geochimica et Cosmochimica Acta, 70, 5571–5582.

――― (2008) Solubility of corundum in the system Al₂O₃-SiO₂-H₂O-NaCl at deep-crustal metamorphic conditions: 800 °C and 10 kbar. Chemical Geology, 249, 250–261.

Newton, R.C., Manning, C.E., Hanchar, J.M., and Finch, R.J. (2005) Gibbs free energy of formation of zircon from measurements of solubility in H₂O. Journal of the American Ceramic Society, 88, 1854–1858.

O'Neill, H.St.C. (1987) Quartz-fayalite-iron and quartz-fayalite-magnetite equilibria and the free energy of formation of fayalite (Fe₂SiO₄) and magnetite (Fe₃O₄). American Mineralogist, 72, 67–75.

――― (2006) Free energy of formation of zircon and hafnon. American Mineralogist, 91, 1134–1141.

Robie, R.A. and Hemingway, B.S. (1995) Thermodynamic properties of minerals and related substances at 298.15 K and 1 bar (10⁵ pascals) pressure and at higher temperatures. U.S. Geological Survey Bulletin, 2131, 461 p.

Robie, R.A., Hemingway, B.S., and Fisher, I.R. (1979) Thermodynamic properties of minerals and related substances at 298.15 K and 1 bar (10⁵ pascals) pressure and at higher temperatures. U.S. Geological Survey Bulletin, 1452, 456 p.

Rosén, E. and Muan, A. (1965) Stability of zircon in the temperature range 1180 to 1366 °C. Journal of the American Ceramic Society, 48, 603–604.

Schuiling, R.D., Vergouwen, L., and Van der Rijst, H. (1976) Gibbs energies of formation of zircon (ZrSiO₄), thorite (ThSiO₄), and phenacite (Be₂SiO₄). American Mineralogist, 61, 166–168.

Tropper, P. and Manning, C.E. (2005) Very low solubility of rutile in H₂O at high pressure and temperature, and its implications for Ti mobility in subduction zones. American Mineralogist, 90, 502–505.

Watson, E.B. and Harrison, T.M. (2005) Zircon thermometer reveals minimum melting conditions on earliest Earth. Science, 308, 841–844.

Watson, E.B., Wark, D.A., and Thomas, J.B. (2006) Crystallization thermometers for zircon and rutile. Contributions to Mineralogy and Petrology, 151, 413–433.

Zhang, Y.G. and Frantz, J.D. (2000) Enstatite-forsterite-water equilibria at elevated temperatures and pressures. American Mineralogist, 85, 918–925.

Zotov, N. and Keppler, H. (2000) In-situ Raman spectra of dissolved silica species in aqueous fluids to 900 °C and 14 kbar. American Mineralogist, 85, 600–603.

――― (2002) Silica speciation in aqueous fluids at high pressures and high temperatures. Chemical Geology, 184, 71–82.